

High Performance Solar Thermoelectric Generator Using Asymmetrical Variable Leg Geometries

Chika Maduabuchi^{1,*}, Kevwe Ejenakevwe^{1,*}, Agwu Nduke¹, and Chigbo Mgbemene¹

¹University of Nigeria Nsukka, Mechanical Engineering Department, Nsukka - Onitsha Rd, Nsukka, Nigeria

Abstract. This paper presents a computational study of the combined effects of variable geometry and asymmetry in the legs of thermocouples of thermoelectric modules used in solar thermoelectric generators (STEGs). Six different models were considered for the thermocouples in each module, namely: rectangular-rectangular legs, rectangular-trapezoidal legs, rectangular-X legs, trapezoidal-trapezoidal legs, trapezoidal-X legs, and X-X legs. Simulations of the six different modules under the same heat flux was carried out in ANSYS 2020 R2 software. Temperature and voltage distributions were obtained for each model and the results indicate significant variations due to the utilization of varying leg geometries. Results show that the X-X leg module generated the highest temperature gradient and electric voltage. In comparison, a temperature gradient and electric voltage of 297 K and 16 V, respectively were achieved with the X-X leg module as against 182 K and 8.4 V, respectively, achieved in a conventional rectangular leg module. This suggests a 63.2% and 90.5% increase in the temperature gradient and electric voltage of the conventional TE module. Therefore, this study demonstrates that X geometry gives the best performance for thermoelectric modules and STEGs.

1 Introduction

Research into improving the performance of a fledging renewable energy technology, solar thermoelectric generators (STEGs), is rapidly gaining interest. This is due to the several attractive features of thermoelectric (TE) devices like being solid state devices & thus frictionless, noiseless, compact, and having little maintenance requirements [1]. However, the conversion efficiency of TE devices, expressed as

* Corresponding authors: chika.maduabuchi.191341@unn.edu.ng, kevwe.itievwe@unn.edu.ng

$$\eta_{TE} = \frac{\Delta T}{T_h} \left(\frac{\sqrt{1 + ZT_m} - 1}{\sqrt{1 + ZT_m} + \frac{T_c}{T_h}} \right) \quad (1)$$

is still not comparable to those of their counterparts like solar photovoltaic, thus giving room for improvement. As seen from eq. (1), one significant way of improving this efficiency is by increasing the temperature gradient, ΔT , across the device. This is also because phenomenologically, TE devices convert thermal energy into electricity through the Seebeck effect. And so, the major driving potential for TE devices is ΔT . Thus, several techniques have been suggested for increasing ΔT . One such technique is the variation of the TE leg geometry.

Several geometries have been studied for TE legs such as trapezoidal, cylindrical, annular, I-legs, Y-legs, X-legs etc. For instance, Al-Merbaty et. al [2] used finite element analysis (FEA) to study the effect of varying pin-leg geometry on the thermal stress, thermal efficiency and power output of a TEG and found that changing the pin geometry improves the efficiency of the device while reducing the maximum stress levels in the pin. They however used fixed hot-side and cold-side temperatures at 513 K and 297 K, respectively, for the simulation, thus giving a ΔT of 215 K. Ali et. al [3] simulated the effect of bi-tapered pin geometry, defined by a dimensionless shape parameter, on the first and second law efficiencies as well as the power output of the device, using energy equation solver (EES). Fixed temperature ratios, $\theta = T_c/T_h$, at 0.3, 0.4, and 0.5, were used for the simulation. They discovered that the dimensionless shape parameter significantly affects the second-law efficiency but only slightly affects the first-law efficiency. Also, that the power output increases with increasing and decreasing values of the shape parameter. Thermodynamic analysis of a TEG was also carried out by Ravita and Kaushik [10] in which they investigated the effect of leg geometry configuration and Thompson effect on the power output and efficiency of the device. Their results showed that a trapezoidal shaped TEG gives a 2.32% and 2.31% increase in energy and exergy efficiency of conventional TEGs, respectively, at $\theta = 0.5$. Validation of these results has also been done by a comparison of simulation results with these and other previous studies in which Yilbas et. al [4] demonstrated a good agreement between their simulation results and results from previous studies. In their study, they simulated the effect of varying temperature at the cold-side of n-type and p-type pins on the efficiency and power output of a TEG with extended pin configuration. The simulation was done using the finite element numerical code ABAQUS. They reported that thermal stress developed in tapered pin configuration attains lower values than that of rectangular pin configuration. Kaushik and Manikandan [5] modelled an annular TEG (ATEG) considering Thompson, Peltier, Joule and Fourier heat conduction effects and did energy and exergy analysis on the model. In their simulation, a fixed value of $T_c = 300$ K was used while T_h was varied from 350 – 600 K. Their analysis revealed that ATEG systems have lower energy/exergy efficiencies as well as power output than conventional TEGs. However, they went on to conclude that ATEG will be more viable in power generation from waste/exhaust heat and solar energy due to its annular shape and higher heat transfer area at its cold-side. This agreed with the recommendation of Shen et al. [6], especially for practical applications with round-shaped heat source/sink. Erturun et. al [7] did a comparative investigation on the thermomechanical and power generation performances of four (4) TEG geometries namely: rectangular, trapezoidal, cylindrical and octagonal geometries. Finite element analysis for two different ΔT (373 K and 573 K) was done using ANSYS. They reported significant differences in the temperature distributions, power outputs and conversion efficiencies of the models due to

varying leg geometries thus demonstrating that varying TE leg geometry can improve the performance of TEGs. However, their results also depicted rectangular legs giving higher efficiency than trapezoidal leg which is contrary to the findings of other studies, thus casting doubt on their results. Similarly, Ibeagwu [8] performed a numerical modelling of the performance of five (5) leg geometries on COMSOL Multiphysics. The geometries had rectangular, trapezoidal, I, Y, and X cross-sectional areas. He also discovered that varying cross-sectional area significantly influences the performance of conventional rect-leg with X-leg being the most efficient and showing a 19.13% increase in power density of the rect-leg. In addition, the X-leg showed the least thermal stresses, while results for the Y and trapezoidal leg predicted possible structural failures before other models. Again, he used fixed values of T_h and T_c at 420 K and 300 K, respectively, for the study.

Attempts have also been made to use different geometries in the thermocouples of TE devices. For example, studies by Liu et al. [9] revealed that a 4.21% increase in power output can be achieved in STEGs with asymmetrical legs. Also, Karana and Sahoo [10] did a theoretical performance analysis of a segmented asymmetrical TEG (SASTEG) and found that nearly 33.3% and 5% increase in current and overall efficiency, respectively, can be achieved for θ of 0.45 – 0.55. Similarly, Shittu et al. [11] conducted a numerical investigation of a SASTEG to optimize its electrical performance and mechanical stability under transient and steady state conditions. Their results showed a 39.21% thermal stress reduction in the asymmetrical leg as compared to the symmetrical leg. Although, they did not use fixed temperatures at the hot- and/or cold-sides like several previous studies did, but instead used rectangular pulsed heat input flux, their study considered just a single cell and not an entire module.

From the review that have been done so far, the feasibility and advantage of variable legs as well as asymmetrical legs has been well established. However, most of these studies focus on just a thermocouple. More so, fixed hot-side and cold-side temperature were considered in most of the studies. Therefore, this study aims to examine the effects of variable legs and asymmetrical legs on an entire TE module rather than just a cell, using heat flux instead of fixed temperatures. Such study is highly relevant as it will give a more realistic guide for the design of STEGs.

2 Methodology

2.1 System description

The proposed thermoelectric geometries considered are presented in Fig. 1. Fig. 1a shows a thermoelectric module (TEM) comprising the conventional rectangular cross-sectional. Fig. 1b and c shows two TEMs made up of rectangular geometries in combination with trapezoidal and X-leg geometries. Similarly, Fig. 1d portrays a TEM comprising trapezoidal leg geometries only, while Fig. 1e depicts a TEM comprising combined trapezoidal and X-leg geometries. Finally, Fig. 1f shows a TEM with X-leg geometries. All TEMs are made up of 127 thermoelements connected electrically in series and thermally in parallel. Incident solar radiation is focused on the TEM top surface, while a convective heat transfer coefficient is assumed at the bottom surface. An electric voltage is generated in the presence of the temperature gradient.

2.2 Numerical Model

The coupled equations governing thermoelectricity are [12,13]

$$\vec{\nabla} \cdot (k \vec{\nabla} T) + J^2 \rho - \tau \vec{J} \cdot \vec{\nabla} T = 0 \quad (2)$$

$$\vec{\nabla} \cdot \left(\xi \vec{\nabla} \frac{\partial V}{\partial t} \right) + \vec{\nabla} \cdot \left(\frac{1}{\rho} \vec{\nabla} V \right) + \vec{\nabla} \cdot (S \vec{\nabla} T) = 0 \quad (3)$$

where S , ρ , k and τ are the temperature dependent Seebeck coefficient, electrical resistivity, thermal conductivity and Thomson coefficient, respectively. \vec{J} is the current density vector. ξ and V are the electric permittivity of the medium and scalar potential of the electric field, respectively.

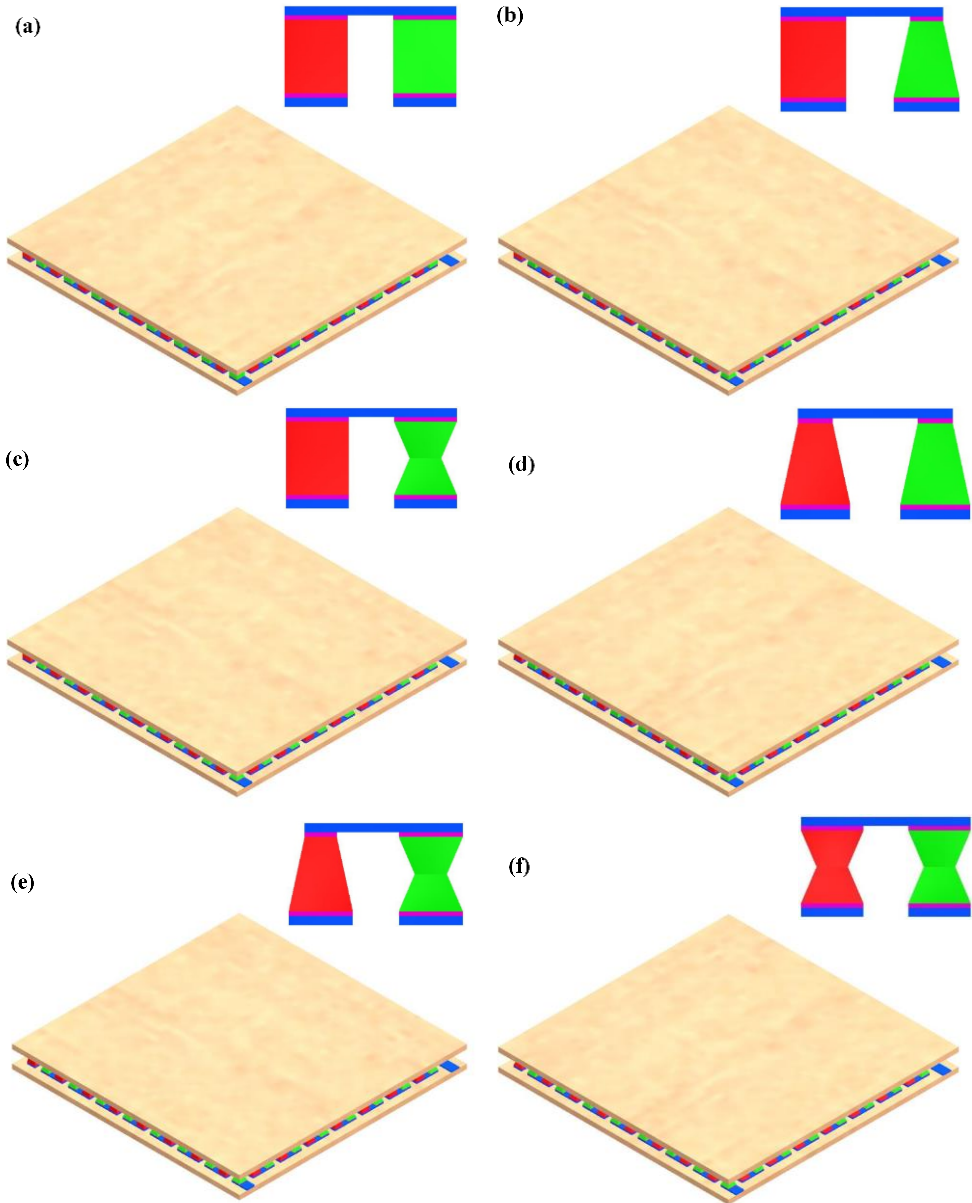


Fig. 1. Proposed models. (a) Case 1 (b) Case 2 (c) Case 3 (d) Case 4 (e) Case 5 (f) Case 6.

3 Results and Discussions

Simulations of the various models was carried out in ANSYS 2020 R2 software with the relevant boundary conditions specified such as the concentrated heat input flux of 50 kW/m^2 at the hot-side and a convective heat transfer coefficient of $500 \text{ W/m}^2\text{K}$ at the cold side. The three-dimensional temperature and voltage distributions obtained are presented in in Figs. 2 and 3, respectively.

From Fig. 2, it can be seen generally that there is a progression in the absorber surface area that is at maximum hot-side temperature as one goes from model 1 to model 6, with virtually the entire absorber surface for model 6 being at maximum hot-side temperature. This implies that the heat flow rates through the TE legs from hot-side to cold-side increases as one goes from model 1 to model 6. Also, for the same heat flux, the maximum hot-side temperature achieved in each model was different with model 1 having the least at 551 K , followed by model 3 at 590 K , then model 2 at 591 K , while models 4, 5, and 6, had the highest at 657 K each. These results show that the temperature gradient is highest in models 4, 5, and 6, and least in model 1. While model 2 has a slightly higher temperature gradient than model 3. Although models 4, 5, and 6 have the same maximum hot-side temperatures, the temperature distribution across the absorber surface further reveals that the total power output would be greater in model 6 followed by model 5 and lastly model 4. This is confirmed by the voltage distribution shown in Fig. 3. Notably, a temperature gradient of 297 K was achieved with model 6 as against 182 K achieved in only a minute fraction of model 1. This suggests a 163.2% increase in the temperature gradient of conventional TE module.

In Fig. 3, it is observed that maximum voltage generated in the STEG increases as one moves from model 1 to model 6, with models 2 and 3 having the same maximum voltage of 11 V , models 4 and 5 having the same maximum voltage of 15 V , and model 6 having the largest maximum voltage of 16 V . This result agrees with the results presented in Fig. 2 and reinforces the inference made from it.

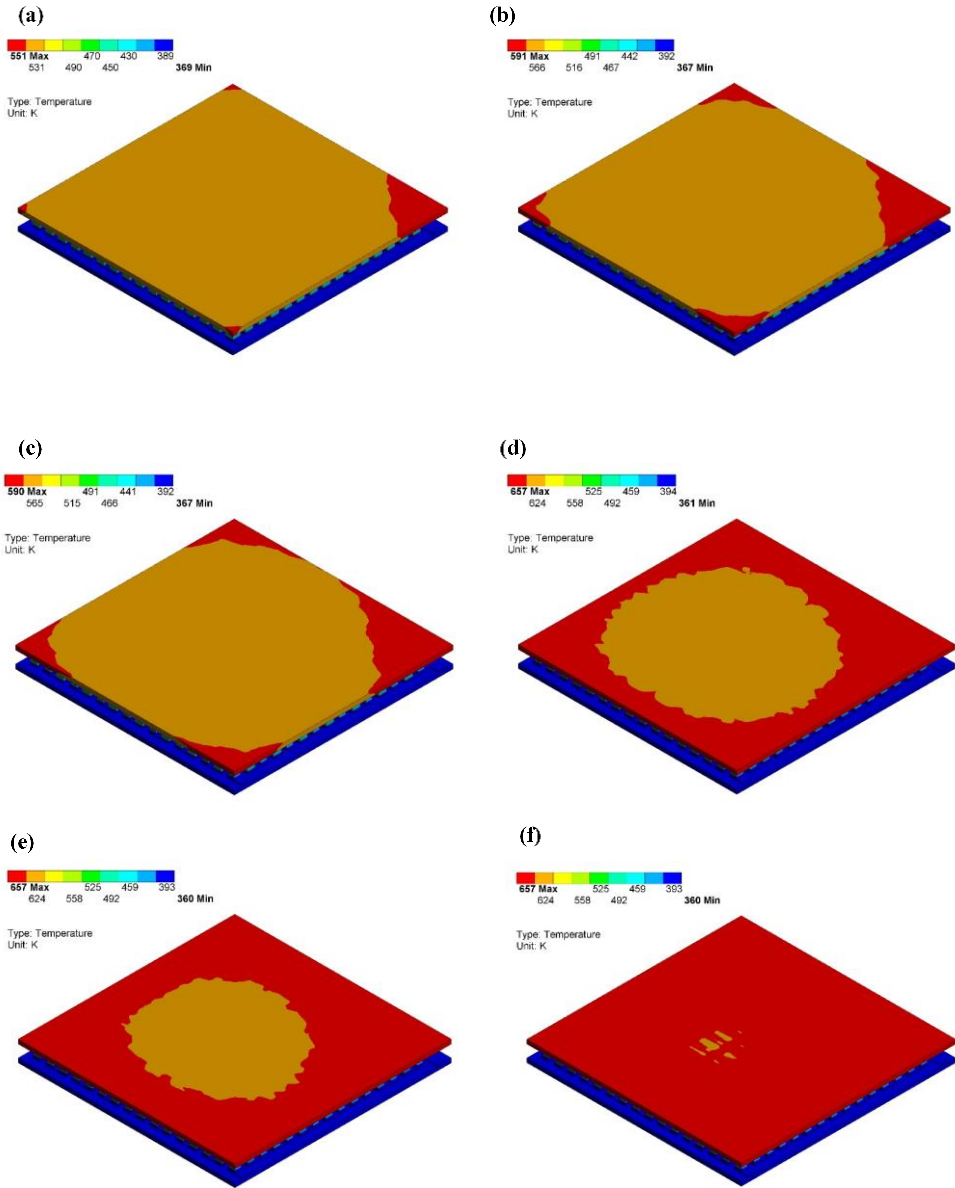


Fig. 2. Temperature distribution. (a) Case 1 (b) Case 2 (c) Case 3 (d) Case 4 (e) Case 5 (f) Case 6.

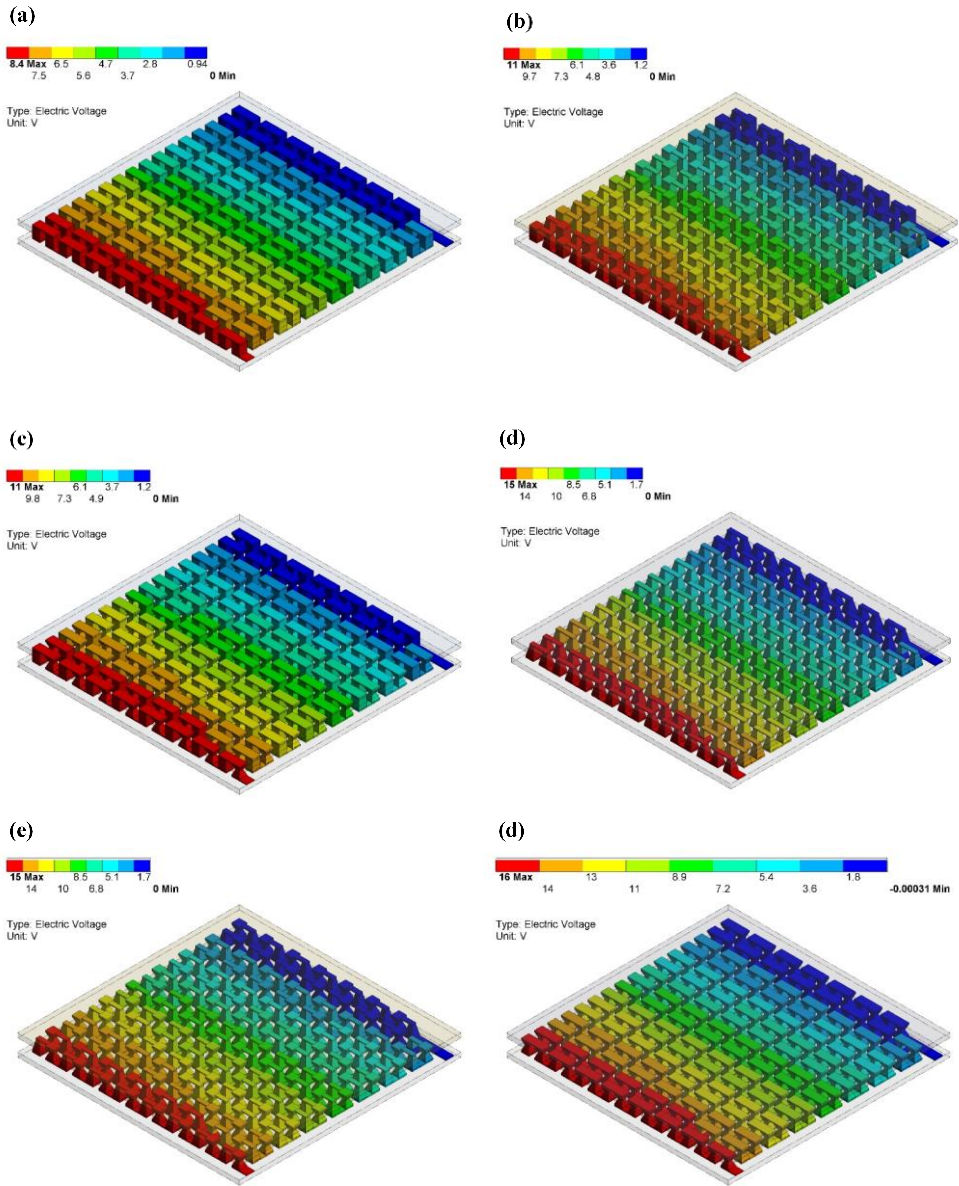


Fig. 3. Voltage distribution. (a) Case 1 (b) Case 2 (c) Case 3 (d) Case 4 (e) Case 5 (f) Case 6.

4 Conclusions

The 3D modelling and simulation of the performance of entire modules for six (6) different STEG models on ANSYS 2020 R2 software was conducted in this study. The models comprise of three (3) symmetrical thermocouples (rect-rect leg, trap-trap leg, and X-X leg) and three (3) asymmetrical thermocouples (rect-trap leg, rect-X leg, and trap-X leg). Standard modules, containing 127 thermocouples was used in the study. For the simulation, the same heat flux (at the hot-side) was specified as boundary condition, which is more realistic than specifying temperatures at boundaries as done in previous studies. Then the temperature and voltage distribution were simulated to see which model performs better.

Overall, the results reveal that model 6, with X-X leg thermocouples, has the best performance in terms of both temperature distribution and voltage distribution. Also, this study has shown that with TE modules composed of thermocouples with homogeneous X-legs, a temperature gradient of 297K can be achieved, which is a 163.2% increase in the temperature gradient for conventional TE modules that consists of only rect-legs. Furthermore, model 6 has equally demonstrated that by fabricating TE modules with only X-legs and applying such for solar based electricity generation, voltages up to 16 V per module can be achieved.

Therefore, this study, through a more realistic approach has further shown the comparative advantage of adopting X cross-sectional area in the design of TE legs. The study is thus highly recommended as a guide for the design and fabrication of TE modules.

References

1. X. F. Zheng, C. X. Liu, Y. Y. Yan, and Q. Wang, *Renew. Sustain. Energy Rev.* **32**, 486 (2014).
2. A. S. Al-Merbati, B. S. S. Yilbas, and A. Z. Z. Sahin, *Appl. Therm. Eng.* **50**, 683 (2013).
3. H. Ali, B. S. Yilbas, and A. Z. Sahin, *Int. J. Exergy* **16**, 53 (2015).
4. B. S. Yilbas, S. S. Akhtar, and A. Z. Sahin, *Energy* **114**, 52 (2016).
5. S. C. Kaushik and S. Manikandan, *Energy Convers. Manag.* **72**, 57 (2015).
6. Z. G. Shen, S. Y. Wu, and L. Xiao, *Energy Convers. Manag.* **89**, 244 (2015).
7. U. Erturun, K. Erermis, and K. Mossi, *Appl. Therm. Eng.* **73**, 126 (2014).
8. O. I. Ibeagwu, *Energy* **180**, 90 (2019).
9. H. B. Liu, J. H. Meng, X. D. Wang, and W. H. Chen, *Energy Convers. Manag.* **175**, 11 (2018).
10. D. R. Karana and R. R. Sahoo, *Energy* **179**, 90 (2019).
11. S. Shittu, G. Li, X. Zhao, X. Ma, Y. Golizadeh, and E. Ayodele, *J. Power Sources* **428**, 53 (2019).
12. C. C. Maduabuchi and C. A. Mgbemene, *J. Electron. Mater.* **49**, 5917 (2020).
13. C. C. Maduabuchi, C. A. Mgbemene, and O. I. Ibeagwu, *J. Electron. Mater.* **1** (2020).